

# The energy-dependent transmission coefficient and the energy distribution of classical particles escaping from a metastable well

Joel S. Bader and B. J. Berne

*Department of Chemistry, Columbia University, New York, New York 10027*

(Received 21 November 1994; accepted 15 February 1995)

We investigate the distribution of energies of thermally activated particles escaping from a metastable well. This energy distribution is connected by detailed balance to the energy-dependent transmission coefficient, the probability that a particle injected into a well will stick. Theoretical expressions for the energy-dependent transmission coefficient show good agreement with simulation results for a one-dimensional reaction coordinate coupled to a frictional bath. Slight deviations from theoretical predictions based on turnover theory [E. Pollak, H. Grabert, and P. Hänggi, *J. Chem. Phys.* **91**, 4073 (1989)] are understood in light of the assumptions of turnover theory. Furthermore, the theoretical expressions for energy distributions also provide good fits for fully three-dimensional simulations of sticking and desorption of Ar and Xe on Pt(111) [J. C. Tully, *Surf. Sci.* **111**, 461 (1981)]. Finally, we compare the theoretical efficiencies of several reactive flux sampling schemes, including a scheme designed to be optimal. © 1995 American Institute of Physics.

## I. INTRODUCTION

Chemical reactions can often be described in terms of a reaction coordinate, or a one-dimensional particle, traveling on a surface with an energetic barrier. The reactant region is on one side of the barrier and the product region is on the other side. At the moment when the particle passes from the reactant region to the product region, it travels with a velocity  $\dot{q}$  which defines a kinetic energy  $\epsilon$ . We concern ourselves with the distribution of energies  $f(\epsilon)$  for thermally activated particles as they pass from reactant to product. The transition state theory of reaction rates and the reactive flux method are presented in terms of  $\epsilon$  in Sec. II A.

The energy distribution of escaping particles serves to probe the frictional damping of the reaction coordinate and is related by detailed balance to the energy-dependent transmission coefficient  $\kappa(\epsilon)$ . The quantity  $\kappa(\epsilon)$  describes the energy dependence of a reaction probability. The sticking probability for atoms in a monoenergetic beam impinging on a surface, e.g., is given by  $\kappa(\epsilon)$ . If frictional damping is small, then particles with a large energy  $\epsilon$  will most likely bounce off of the surface. If the damping is large, then particles with large energy will be more likely to stick than particles with small energies. In Sec. II B we present an expression for  $\kappa(\epsilon)$  for a parabolic barrier, which is also valid for escape over nonlinear barriers when the frictional damping is moderate to strong. When the motion of the reaction coordinate is only weakly damped, another expression based on turnover theory and described in Sec. II C is appropriate. Interpolation formulas connecting the weak friction and strong friction limits for  $\kappa(\epsilon)$  are presented in Sec. II D. Formulas are also presented for the energy distribution of escaping particles,  $f(\epsilon)$ , and for the first moment of  $f(\epsilon)$ ,  $\bar{\epsilon}$ , which is the mean energy of an escaping particle as it crosses the transition state dividing surface.

We show in Sec. III A that the theory developed for a one-dimensional reaction coordinate can be successfully applied to the fully three-dimensional sticking of Ar and Xe atoms on a Pt(111) surface. Theoretical expressions agree

well with simulation results for sticking probabilities of monoenergetic and thermal beams, and with results for the average energies of thermally desorbing particles.<sup>1</sup>

The energy distribution  $f(\epsilon)$  is the central quantity of the Pollak–Grabert–Hänggi (PGH) turnover theory for condensed phase reaction rates, which has been quite successful in predicting rate constants for systems with weak friction, strong friction, and for the crossover region between weak and strong friction too.<sup>2,3</sup> The PGH rate expressions involve integrals over  $f(\epsilon)$ . We test PGH theory at a microscopic level by comparing the theoretically predicted value for  $f(\epsilon)$  with the actual value obtained by simulation. The simulation tests are reported in Sec. III B. The results bring to light an intriguing cancellation of errors in the calculation of a transmission coefficient based on the PGH prediction for  $f(\epsilon)$ .

We also use theoretical expressions for the energy-dependent transmission coefficient to investigate the relative efficiencies of various reactive flux sampling schemes. One common scheme is to select the initial velocity of the reaction coordinate from a Boltzmann distribution; another is to select the initial velocity from a Maxwell–Boltzmann flux distribution. In Sec. III C, the efficiencies of these schemes are compared with the efficiency for sampling from the optimal distribution, the distribution which produces the best estimate for  $\kappa$  with the smallest number of trajectories. The optimal distribution is described in the limits of strong friction and weak friction. Sampling from the optimal distribution is shown to converge faster than sampling from the Boltzmann and Maxwellian flux distribution, and for very weak friction the difference can be significant.

In Sec. IV we conclude with a discussion highlighting the findings of our study. We discuss in particular why the errors made by PGH theory tend to be in compensating directions, leading in the end to very accurate predictions of reaction rates. We also describe possible extensions to the work presented here.

## II. THEORY

### A. Reactive flux in the energy representation

We take a standard model for the dynamics of a particle escaping from a metastable well, namely the generalized Langevin equation (GLE),<sup>4-6</sup>

$$\mu \ddot{q}(t) = -\frac{dV(q)}{dq} - \mu \int_0^t dt' \gamma(t-t') \dot{q}(t') + \xi(t). \quad (1)$$

The reaction coordinate is  $q$ , and  $\mu$  is the mass of the reaction coordinate. The potential of mean force,  $V(q)$ , is assumed to have a barrier of height  $V^\ddagger$  at  $q=q^\ddagger$ . The barrier separates reactants,  $q < q^\ddagger$ , from products,  $q > q^\ddagger$ . For convenience, we take  $q^\ddagger = 0$ .

The coordinate is coupled to a thermal bath by means of a Gaussian random force  $\xi(t)$  and a friction kernel  $\gamma(t)$ . The friction kernel is related to the random force autocorrelation function by a fluctuation-dissipation theorem,

$$\langle \xi(t) \xi(t') \rangle = k_B T \mu \gamma(|t-t'|). \quad (2)$$

The random force has zero mean,  $\langle \xi(t) \rangle = 0$ , and is uncorrelated with  $q$ ,  $\langle \xi(t) q(t') \rangle = 0$  for  $t \geq t'$ .

Our analysis of the energy distribution of reactive particles is framed in terms of the reactive flux theory for barrier crossing.<sup>7-13</sup> The reactive flux method has as its starting point the transition state theory estimate for the rate constant  $k_{\text{tst}}$  for thermal escape from the reactant region,

$$k_{\text{tst}} = \langle \delta(q) \dot{q} \Theta[\dot{q}] \rangle / \langle \Theta[-q] \rangle. \quad (3)$$

The function  $\Theta$  is the Heaviside function.

The transition state theory rate constant does not account for recrossings of the transition state by an activated particle before it is thermalized in the reactant region or product region. The ratio of the actual rate constant  $k$  to the transition state theory estimate  $k_{\text{tst}}$  is termed the transmission coefficient  $\kappa$ . It is possible to obtain the value of  $\kappa$  by running trajectories away from the transition state dividing surface for a time  $\tau$ , where  $\tau$  is long enough that the system has thermalized in the reactant or product region but not so long that it can become reactivated. When this separation of time scales exists, the transmission coefficient is

$$\kappa = \frac{\langle \delta(q) \dot{q} \Theta[q(\tau)] \rangle}{\langle \delta(q) \dot{q} \Theta[\dot{q}] \rangle}. \quad (4)$$

Writing the average explicitly in terms of the initial  $\dot{q}$ ,

$$\kappa = \frac{\int_{-\infty}^{\infty} d\dot{q} e^{-\beta \mu \dot{q}^2 / 2} \dot{q} \langle \Theta[q(\tau; \dot{q})] \rangle_{\xi}}{\int_{-\infty}^{\infty} d\dot{q} e^{-\beta \mu \dot{q}^2 / 2} \dot{q} \Theta[\dot{q}]}. \quad (5)$$

The position of the trajectory starting from  $q^\ddagger$  with velocity  $\dot{q}$  after the plateau time  $\tau$  is  $q(\tau; \dot{q})$ . The average over histories of the random force  $\xi(t)$  is denoted by  $\langle \dots \rangle_{\xi}$ .

Rather than retaining the velocity  $\dot{q}$  to characterize the initial conditions, we choose to write  $\kappa$  in terms of the energy of  $q$ , relative to the barrier energy, as it moves away from the barrier at time zero. This energy in units of  $k_B T$  is  $\epsilon = \beta \mu \dot{q}^2 / 2$ . In terms of  $\epsilon$ , the transmission coefficient is

$$\kappa = \int_0^{\infty} d\epsilon e^{-\epsilon} \kappa(\epsilon). \quad (6)$$

An important quantity related to  $\kappa(\epsilon)$  is  $f(\epsilon)$ , the energy distribution of particles leaving the reactant region. By detailed balance, the normalized distribution is

$$f(\epsilon) = \kappa^{-1} e^{-\epsilon} \kappa(\epsilon). \quad (7)$$

In Eq. (6) we have introduced the energy-dependent transmission coefficient  $\kappa(\epsilon)$ , defined as

$$\kappa(\epsilon) = \langle \Theta[q(\tau; \sqrt{2\epsilon k_B T / \mu})] \rangle_{\xi} - \langle \Theta[q(\tau; -\sqrt{2\epsilon k_B T / \mu})] \rangle_{\xi}. \quad (8)$$

As seen in Eq. (6), the Boltzmann weighted average of the energy-dependent transmission coefficient  $\kappa(\epsilon)$  yields the conventional transmission coefficient. Although  $\kappa(\epsilon)$  specifies an initial energy for the reactive system, it is not a microcanonical quantity because coupling with the bath allows energy transfer into and out of the reaction coordinate. The quantity  $\epsilon$  specifies how the reactive coordinate  $q$  is prepared at the top of the barrier, i.e., how much kinetic energy it possesses as it crosses the transition state dividing surface at  $t=0$ .

One quantity we wish to calculate is  $\bar{\epsilon}$ , the average energy of reactive particles, relative to the barrier top energy, at the moment when  $q = q^\ddagger$ :

$$\bar{\epsilon} = \frac{\langle \delta(q) \dot{q} \Theta[q(\tau)] \epsilon \rangle}{\langle \delta(q) \dot{q} \Theta[q(\tau)] \rangle}. \quad (9)$$

The unsubscripted variables  $q$ ,  $\dot{q}$ , and  $\epsilon$  refer to the position, velocity, and reduced energy at time zero. In terms of  $\kappa(\epsilon)$ , the average energy of escaping particles is

$$\bar{\epsilon} = \kappa^{-1} \int_0^{\infty} d\epsilon e^{-\epsilon} \kappa(\epsilon) \epsilon. \quad (10)$$

It is convenient to use Laplace transforms of  $\kappa(\epsilon)$  to relate the overall transmission coefficient  $\kappa$  and the average escape energy  $\bar{\epsilon}$  to  $\kappa(\epsilon)$ . Defining the Laplace transform of  $\kappa(\epsilon)$  as  $\tilde{\kappa}(s)$ ,

$$\tilde{\kappa}(s) = \int_0^{\infty} d\epsilon e^{-s\epsilon} \kappa(\epsilon), \quad (11)$$

the transmission coefficient and the average escape energy are

$$\kappa = \tilde{\kappa}(s)|_{s=1}, \quad (12)$$

$$\bar{\epsilon} = -\frac{d}{ds} \ln \tilde{\kappa}(s) \Big|_{s=1}. \quad (13)$$

Indeed, all moments of the distribution  $\kappa(\epsilon)$  can be obtained by suitable differentiation of the generating function  $\tilde{\kappa}(s)$ . The variance, characterizing the width of the distribution of energies of escaping particles, is

$$\langle \epsilon^2 \rangle - \bar{\epsilon}^2 = \frac{d^2}{ds^2} \ln \tilde{\kappa}(s) \Big|_{s=1}. \quad (14)$$

### B. Escape over a parabolic barrier

It is possible to calculate  $\kappa(\epsilon)$  in a simple closed form when the barrier  $V(q)$  is parabolic. The form of  $\kappa(\epsilon)$  for a parabolic barrier should also be accurate when the frictional damping is large and the dynamics of activated particles are dominated by motion close to a parabolic barrier top. For a parabolic barrier with imaginary frequency  $\omega^\ddagger$ , the GLE of Eq. (1) is

$$\ddot{q}(t) = \omega^{\ddagger 2} q(t) + \mu^{-1} \xi(t) - \int_0^t dt' \gamma(t-t') \dot{q}(t'). \quad (15)$$

The linear dynamics of the GLE can be posed in terms of a harmonic Hamiltonian. Normal mode analysis of the Hamiltonian can be employed to obtain the transmission coefficient  $\kappa$ .<sup>14</sup> It is also possible to obtain  $\kappa$  without recourse to an explicit harmonic Hamiltonian, but with the equivalent requirement that the stochastic force  $\xi(t)$  be a Gaussian random process.<sup>13,15,16</sup> Here we use similar means to obtain  $\kappa(\epsilon)$ . The starting point is the Laplace transform of Eq. (15),

$$\tilde{q}(s) = \frac{\dot{q} + \mu^{-1} \tilde{\xi}(s)}{\Delta(s)}, \quad (16)$$

where  $\tilde{q}(s) = \int_0^\infty dt e^{-st} q(t)$  and  $\Delta(s) = s^2 + s \tilde{\gamma}(s) - \omega^{\ddagger 2}$ . The initial conditions are  $\dot{q}(0) = \dot{q}$  and  $q(0) = q^\ddagger = 0$ . The Laplace transform of the random force is  $\tilde{\xi}(s)$ .

At long times, the largest positive root  $\lambda^\ddagger$  of the equation  $\Delta(s) = 0$  dominates the inverse Laplace transform for  $q(t)$ . This root, termed  $\lambda^\ddagger$ , is the Grote–Hynes frequency,<sup>14,17,18</sup>

$$\lambda^\ddagger = \frac{\omega^{\ddagger 2}}{\lambda^\ddagger + \tilde{\gamma}(\lambda^\ddagger)}. \quad (17)$$

Thus  $q(t)$  is given asymptotically by

$$q(t) \sim e^{\lambda^\ddagger t} \lim_{s \rightarrow \lambda^\ddagger} \left[ \frac{s - \lambda^\ddagger}{\Delta(s)} \right] \{ \dot{q} + \mu^{-1} \tilde{\xi}(s) \}. \quad (18)$$

In Appendix A we describe why there must be a positive root and show that the term in square brackets,  $[(s - \lambda^\ddagger)/\Delta(s)]$ , is positive as  $s \rightarrow \lambda^\ddagger$ .

Consequently  $q(t)$  will be in the product region at long times only if  $\tilde{\xi}(\lambda^\ddagger)$  is larger than  $-\mu \dot{q}$ . Therefore  $\kappa(\epsilon)$  depends on the bath solely through the probability distribution  $P[\tilde{\xi}(\lambda^\ddagger)]$  for  $\tilde{\xi}(\lambda^\ddagger)$ , since

$$\langle \Theta[q(\tau; \dot{q})] \rangle_\xi = \int_{-\mu \dot{q}}^\infty d\tilde{\xi}(\lambda^\ddagger) P[\tilde{\xi}(\lambda^\ddagger)]. \quad (19)$$

Furthermore, since  $\xi(t)$  is a Gaussian random variable,  $\tilde{\xi}(\lambda^\ddagger)$  also has a Gaussian distribution,

$$P[\tilde{\xi}(\lambda^\ddagger)] = \frac{1}{\sqrt{2\pi \langle \tilde{\xi}(\lambda^\ddagger)^2 \rangle}} \exp \left[ -\frac{\tilde{\xi}(\lambda^\ddagger)^2}{2 \langle \tilde{\xi}(\lambda^\ddagger)^2 \rangle} \right]. \quad (20)$$

The width of the Gaussian distribution is

$$\begin{aligned} \langle \tilde{\xi}(\lambda^\ddagger)^2 \rangle &= \int_0^\infty dt_1 \int_0^\infty dt_2 e^{-\lambda^\ddagger(t_1+t_2)} \langle \xi(t_1) \xi(t_2) \rangle \\ &= 2 \int_0^\infty dt_1 e^{-2\lambda^\ddagger t_1} \int_{t_1}^\infty dt_2 e^{-\lambda^\ddagger(t_2-t_1)} \\ &\quad \times \langle \xi(0) \xi(t_2-t_1) \rangle \\ &= \frac{\mu \tilde{\gamma}(\lambda^\ddagger)}{\beta \lambda^\ddagger}. \end{aligned} \quad (21)$$

With these observations, Eq. (8) becomes

$$\kappa(\epsilon) = \text{erf} \left[ \sqrt{\epsilon \lambda^\ddagger / \tilde{\gamma}(\lambda^\ddagger)} \right], \quad (22)$$

where  $\text{erf}(x) = 2\pi^{-1/2} \int_0^x dt e^{-t^2}$ . Inserting Eq. (22) for  $\kappa(\epsilon)$  into Eq. (11) and exchanging the order of integration for the erf and  $\epsilon$ , we obtain

$$\tilde{\kappa}(s) = s^{-1} [1 + s \tilde{\gamma}(\lambda^\ddagger) / \lambda^\ddagger]^{-1/2}. \quad (23)$$

Setting  $s = 1$ , the Grote–Hynes expression for the transmission coefficient is obtained,<sup>14,17,18</sup>

$$\kappa = \left[ 1 + \frac{\tilde{\gamma}(\lambda^\ddagger)}{\lambda^\ddagger} \right]^{-1/2} = \frac{\lambda^\ddagger}{\omega^{\ddagger 2}} = \kappa_{\text{pb}}. \quad (24)$$

The subscript ‘‘pb’’ stands for parabolic barrier, since this expression is exact when the barrier is an inverted parabola.

Differentiating with respect to  $s$  and making use of the relationship in Eq. (24), the average energy of escaping particles is

$$\bar{\epsilon} = 1 + \frac{\lambda^\ddagger \tilde{\gamma}(\lambda^\ddagger)}{2 \omega^{\ddagger 2}} = \frac{3}{2} - \frac{1}{2} \left( \frac{\lambda^\ddagger}{\omega^{\ddagger 2}} \right)^2. \quad (25)$$

This expression is exact for a parabolic barrier. Furthermore, it should be reasonably accurate when motion near the barrier top decides the fate of activated particles, i.e., in the regime of moderate to large damping. When the damping is moderate,  $\lambda^\ddagger \approx \omega^\ddagger$ , and reactive particles cross the barrier with about  $1 k_B T$  of energy. The result  $\bar{\epsilon} = 1$  is exactly the prediction of transition state theory. It results from the assumption that particles crossing the transition state are drawn from an equilibrium distribution, and that there are no rapid recrossings of the transition state dividing surface. As the damping becomes larger, the frictional forces cause recrossings of the transition state. Recrossings are less likely as the initial kinetic energy increases, and  $\bar{\epsilon}$  increases with friction, rising above the transition state theory estimate of  $1 k_B T$  and eventually saturating at  $(3/2) k_B T$ . The value at saturation is estimated using the limiting results for large friction,  $\lambda^\ddagger \approx \omega^{\ddagger 2} / \tilde{\gamma}(\lambda^\ddagger) \ll \omega^\ddagger$ . Although the average energy of an escaping particle in the high friction limit is  $(3/2) k_B T$  as the particle crosses the barrier, the energy should be rapidly thermalized by the frictional coupling and return to the equilibrium value as the particle moves away from the barrier.

We take a second derivative of Eq. (23) to find the variance of the distribution,

$$\langle \epsilon^2 \rangle - \bar{\epsilon}^2 = 1 + \frac{1}{2} \left[ \frac{\lambda^\ddagger \tilde{\gamma}(\lambda^\ddagger)}{\omega^{\ddagger 2}} \right]^2. \quad (26)$$

For moderate friction, the variance approaches unity. This is because  $\kappa(\epsilon)$  approaches 1 for all values of  $\epsilon$ , just the result of transition state theory. As friction increases, the variance increases as well. At very high friction, the term in square brackets in Eq. (26) approaches 1, and the variance saturates at the high friction limit of 3/2.

As the frictional damping increases, the number of diffusive recrossings of the transition state dividing surface increases. The recrossings decrease the transmission coefficient  $\kappa$  and the energy-dependent transmission coefficient  $\kappa(\epsilon)$ . Although  $\kappa(\epsilon)$  decreases, the normalized energy distribution of escaping particles,  $f(\epsilon) = \kappa^{-1} \exp(-\epsilon)\kappa(\epsilon)$ , approaches a limiting form. Expanding the error function in the definition of  $\kappa(\epsilon)$  to lowest order in its argument,

$$f(\epsilon) = \exp(-\epsilon) \left[ 1 + \frac{\tilde{\gamma}(\lambda^\ddagger)}{\lambda^\ddagger} \right]^{1/2} \frac{2}{\sqrt{\pi}} \times \left\{ \sqrt{\epsilon \frac{\lambda^\ddagger}{\tilde{\gamma}(\lambda^\ddagger)}} + \mathcal{O}\left(\frac{\lambda^\ddagger}{\tilde{\gamma}(\lambda^\ddagger)}\right)^{3/2} \right\} = \frac{2}{\sqrt{\pi}} \exp(-\epsilon) \epsilon^{1/2} + \mathcal{O}(\kappa^2). \quad (27)$$

The error in this expansion is of order  $[\lambda^\ddagger/\tilde{\gamma}(\lambda^\ddagger)] \sim [\omega^\ddagger/\tilde{\gamma}(\lambda^\ddagger)]^2 \sim \kappa^2$ . To  $\mathcal{O}(\kappa^2)$ , the  $n$ th moment of the distribution of energies of escaping particles can be obtained from the asymptotic distribution, Eq. (27):

$$\langle \epsilon^n \rangle = \frac{2}{\sqrt{\pi}} \int_0^\infty d\epsilon \exp(-\epsilon) \epsilon^{n+1/2} = 2 \cdot \frac{1}{2} \cdot \frac{3}{2} \cdot \dots \cdot \frac{2n+1}{2}. \quad (28)$$

### C. Weak friction and energy diffusion

So far we have discussed the energy in terms of the reaction coordinate  $q$ . It has been shown explicitly, however, that the generalized Langevin equation for a parabolic barrier, Eq. (15), is identical to separable motion for a rotated set of oscillators.<sup>5,14</sup> One of these barrier-top normal modes is unstable. The unstable barrier-top normal mode is termed  $\rho$ , and its imaginary frequency  $\lambda^\ddagger$  is the Grote-Hynes frequency. For a metastable well, the normal modes obtained from a quadratic expansion at the barrier-top mix with each other away from the barrier region, causing an exchange of energy between the unstable mode  $\rho$  and the remaining degrees of freedom.

In the weak friction limit, slow energy diffusion between the unstable mode  $\rho$  and the rest of the system serves to decrease the reaction rate below  $k_{\text{tst}}$ . The kernel  $P(\epsilon'|\epsilon)$  characterizes the exchange of energy between  $\rho$  and the remaining modes. The probability that the unstable mode  $\rho$ , having energy  $\epsilon$  when it moves away from the barrier and into the metastable well, will return to the barrier with an energy between  $\epsilon'$  and  $\epsilon' + d\epsilon$  is  $P(\epsilon'|\epsilon)d\epsilon$ . It is convenient to characterize  $P(\epsilon'|\epsilon)$  by its first and second moment. It is

also usual to assume that  $P(\epsilon'|\epsilon)$  is only required for energies near the barrier-top energy, and therefore that  $P(\epsilon'|\epsilon)$  depends only on the difference  $\epsilon' - \epsilon$ . The form for the kernel satisfying these requirements and detailed balance is<sup>2,3,19</sup>

$$P(\epsilon'|\epsilon) = \frac{1}{\sqrt{4\pi\delta}} \exp[-(\epsilon' + \delta - \epsilon)^2/4\delta]. \quad (29)$$

The average energy loss in units of  $k_B T$  for the mode  $\rho$  when it starts at the barrier energy is termed  $\delta$ , and the variance in the reduced energy after a transit of the metastable well is  $2\delta$ .

When friction is weak, the unstable mode  $\rho$  is almost identical to the reaction coordinate  $q$ , and  $\delta$  can be estimated from the dynamics of  $q$  rather than the more complicated dynamics of  $\rho$ .<sup>2,3,19</sup> To lowest order in the frictional damping and the inverse of the barrier height  $1/\beta V^\ddagger$ , the energy loss is

$$\delta = \frac{\beta\mu}{2} \int_{-T}^T dt_1 \int_{-T}^T dt_2 \dot{q}(t_1) \gamma(t_1 - t_2) \dot{q}(t_2). \quad (30)$$

The asymptotic undamped trajectory  $q(t)$  starts at the barrier in the infinite past with energy  $\epsilon \rightarrow 0$ , traverses the metastable well once, and returns to the barrier top at time  $T \rightarrow \infty$ .

Particles escape from the metastable well with a rate constant  $k$ ,<sup>2,3,6</sup>

$$k = k_{\text{tst}} \kappa_{\text{pb}} \kappa_\rho, \quad (31a)$$

where

$$k_{\text{tst}} = (\omega_0/2\pi) \exp[-\beta V^\ddagger], \quad (31b)$$

$$\kappa_{\text{pb}} = \lambda^\ddagger/\omega^\ddagger, \quad (31c)$$

and

$$\kappa_\rho = \exp\left\{ \frac{1}{2\pi} \int_{-\infty}^{\infty} dx \frac{\ln[1 - \exp(-\delta x^2 - \delta/4)]}{x^2 + 1/4} \right\}. \quad (31d)$$

The frequencies  $\omega_0$  and  $\omega^\ddagger$  correspond to the curvature of  $V(q)$  at the well and at the barrier, and  $\lambda^\ddagger$  is the Grote-Hynes frequency defined in Eq. (24).

The energy-dependent transmission coefficient  $\kappa_\rho(\epsilon)$  for the unstable mode  $\rho$  can be obtained by noting that the steady-state distribution of particles leaving the well per unit energy and unit time, normalized to one particle in the well, is  $F(\epsilon) = \exp(-\epsilon) k_{\text{tst}} (\lambda^\ddagger/\omega^\ddagger) \kappa_\rho(\epsilon)$ . The distribution  $F(\epsilon)$  is the solution to the integral equation,<sup>2,3</sup>

$$F(\epsilon) = \int_{-\infty}^0 d\epsilon' P(\epsilon|\epsilon') F(\epsilon') \quad (32)$$

with the additional boundary condition  $\kappa_\rho(\epsilon) \rightarrow 1$  as  $\epsilon \rightarrow -\infty$ . The solution of Eq. (32) is<sup>2</sup>

$$\kappa_\rho(\epsilon) = \exp[(A + 1/2)\epsilon] G^{-1} \left( -\frac{i}{2} \right) \frac{1}{\pi} \times \int_0^\infty d\lambda \frac{R(\lambda, A)}{\lambda^2 + (A + 1/2)^2} \times \{ [A + 1/2] \cos[\lambda\epsilon + \theta(\lambda, A)] + \lambda \sin[\lambda\epsilon + \theta(\lambda, A)] \}. \quad (33)$$

In this equation,

$$G^{-}\left(-\frac{i}{2}\right)=\exp\left\{\frac{1}{2\pi}\int_0^{\infty}d\lambda\frac{\ln G(\lambda)}{\lambda^2+1/4}\right\}=R(0,1/2); \quad (35)$$

$$R(\lambda,A)=\exp\left\{\frac{1}{2\pi}\int_0^{\infty}dy\left[\frac{A}{(\lambda-y)^2+A^2}+\frac{A}{(\lambda+y)^2+A^2}\right]\ln G(y)\right\}; \quad (36)$$

$$\theta(\lambda,A)=\exp\left\{\frac{1}{2\pi}\int_0^{\infty}dy\frac{y}{y^2+A^2}[\ln G(\lambda+y)-\ln G(\lambda-y)]\right\}; \quad (37)$$

the arbitrary constant  $A$  is real and non-negative; and  $G(\lambda)=1-\exp[-\delta(\lambda^2+1/4)]$ . In the limit of large  $\lambda$ ,  $R(\lambda,A)\rightarrow 1$  and  $\theta(\lambda,A)\rightarrow 0$ . Therefore, the integrand in Eq. (34) approaches  $[(A+1/2)\cos(\lambda\epsilon)+\lambda\sin(\lambda\epsilon)]/[\lambda^2+(A+1/2)^2]$  for large  $\lambda$ . For numerical evaluation, we found it advantageous to perform this slowly convergent part of the integral analytically. The remainder of the integral was computed numerically with routines from the QUADPACK library.<sup>20</sup> In our calculations we chose  $A\rightarrow 0^+$ , giving  $R(\lambda,A)=\sqrt{G(\lambda)}$ .

The average energy of the unstable mode when it crosses the barrier top is termed  $\bar{\epsilon}_\rho$ . The subscript  $\rho$  serves to distinguish this energy from that of the reaction coordinate  $\bar{\epsilon}$ . Equivalent expressions for the normal mode energy  $\bar{\epsilon}_\rho$  valid over the entire damping range are<sup>2,21,22</sup>

$$\bar{\epsilon}_\rho=1+\frac{1}{\pi}\int_0^{\infty}dx\ln\left[1-e^{-\delta(x^2+1/4)}\right]\frac{-x^2+1/4}{[x^2+1/4]^2} \quad (38)$$

$$=1+\frac{2}{\pi}\int_0^{\pi/2}dy\ln\left[1-e^{-\delta/(4r\cos^2y)}\right](2\cos^2y-1). \quad (39)$$

#### D. Interpolation formulas

When friction is moderate to large, transition state theory is virtually exact for the unstable mode escape dynamics and  $\bar{\epsilon}_\rho$  approaches 1 exponentially quickly.<sup>2</sup> This is in contrast to the behavior of the average energy for the reaction coordinate  $\bar{\epsilon}\rightarrow 3/2$  for large friction.

When friction is small, the unstable mode  $\rho$  is (within a mass scaling) virtually identical to the reaction coordinate  $q$ . Thus, when friction is small,  $\bar{\epsilon}_\rho\approx\bar{\epsilon}$ . Furthermore,  $\bar{\epsilon}_\rho\sim\sqrt{\delta}\ll 1$ . This suggests an interpolation formula for  $\bar{\epsilon}$  in terms of  $\bar{\epsilon}_\rho$ . The formula is obtained by replacing the weak friction limit of Eq. (25),  $\bar{\epsilon}=1$ , with the correct limit  $\bar{\epsilon}=\bar{\epsilon}_\rho$ , yielding

$$\bar{\epsilon}=\bar{\epsilon}_\rho+\frac{\lambda^\ddagger\tilde{\gamma}(\lambda^\ddagger)}{2\omega^\ddagger{}^2}. \quad (40)$$

This formula bridges between the strong damping limit, when diffusive motion near the barrier top influences the rate

of escape, and the weak damping limit, where energy diffusion between the reaction coordinate and the bath is rate limiting.

It is also possible to construct an interpolation formula for  $\kappa(\epsilon)$  itself to bridge the weak damping and large damping limits. An interpolation formula suggested by the rigorous result<sup>3</sup>  $\kappa=\kappa_{\text{pb}}\kappa_\rho$  is

$$\kappa(\epsilon)=\kappa_{\text{pb}}(\epsilon)\kappa_\rho(\epsilon). \quad (41)$$

This interpolation formula is motivated in a manner similar to that of Eq. (40). The first term,  $\kappa_{\text{pb}}(\epsilon)$ , is the energy-dependent transmission coefficient from Eq. (22). This term is the exact result for  $\kappa(\epsilon)$  for a parabolic barrier; it gives  $\kappa(\epsilon)$  correctly for escape from a metastable well when the frictional damping is moderate to large. In the weak damping limit,  $\kappa_{\text{pb}}(\epsilon)$  approaches the transition state theory value of 1. The second term,  $\kappa_\rho(\epsilon)$ , is the transmission coefficient for the unstable mode. For moderate to large damping, transition state theory is valid and this quantity approaches 1. In the weak damping limit, inertial recrossings decrease the transmission coefficient. Since the reaction coordinate and the unstable normal mode are essentially identical when friction is small,  $\kappa(\epsilon)$  is given by  $\kappa_\rho(\epsilon)$  in the weak damping limit.

We note that Eq. (41) is not exactly correct, since

$$\begin{aligned} \kappa &= \kappa_{\text{pb}}\kappa_\rho \\ &= \int_0^\infty d\epsilon e^{-\epsilon}\kappa_{\text{pb}}(\epsilon) \int_0^\infty d\epsilon' e^{-\epsilon'}\kappa_\rho(\epsilon') \\ &\neq \int_0^\infty d\epsilon e^{-\epsilon}\kappa_{\text{pb}}(\epsilon)\kappa_\rho(\epsilon). \end{aligned}$$

One measure of the error one makes with the interpolation formula  $\kappa(\epsilon)=\kappa_{\text{pb}}(\epsilon)\kappa_\rho(\epsilon)$  is to compare  $\int_0^\infty d\epsilon e^{-\epsilon}\kappa_{\text{pb}}(\epsilon)\kappa_\rho(\epsilon)$  with the exact value for  $\kappa$  given by Eqs. (31a)–(31d). For the systems for which we provide simulation results, the relative difference between these two quantities was less than 1%. We consider this to be a negligible error.

### III. APPLICATIONS

#### A. Sticking probabilities and thermal desorption

The theoretical expressions developed in Sec. II can be used to obtain a more complete understanding of sticking probabilities  $P_{\text{stick}}$  for atoms impinging on a surface. By detailed balance, the sticking probability is related to the thermal desorption rate  $k_D$  by  $k_D=P_{\text{stick}}k_{\text{TST}}$ , where  $k_{\text{TST}}$  is the transition state theory estimate for the thermal desorption rate. A similar detailed balance relationship exists between the dependence of  $P_{\text{stick}}$  on the incident energy  $E_0$  of a particle approaching a surface and the distribution of energies of particles thermally desorbing from a surface.

In a fully three-dimensional description of the particle and surface,  $P_{\text{stick}}$  can depend on the angle of incidence  $\theta$  of the particle with respect to the surface normal. If the reaction coordinate for adsorption is effectively one-dimensional,  $P_{\text{stick}}$  should depend only on the energy in the normal direction,  $E_0\cos^2\theta$ . Generally, normal energy scaling can only be

expected for a perfectly flat surface which does not couple motion in the normal direction to motion in the plane parallel to the surface.

We investigate the ability of our one-dimensional theory to describe the energy and temperature dependence of  $P_{\text{stick}}$  for a fully three-dimensional model of rate gas atoms interacting with a surface, where motion in all three dimensions is coupled by the surface corrugation. The simulation results we discuss were reported by Tully for a model of isolated Ar and Xe atoms interacting with the Pt(111) surface.<sup>1</sup>

The rare gas atom in Tully's simulation interacted by a pairwise Lennard-Jones potential with the closest 14 atoms on the Pt surface. The interactions with the remaining atoms were included using a continuum term dependent on the height of the rare gas atom above the surface. The four surface atoms closest to the rare gas atom were allowed to move, and the identity of these four atoms followed the shadow the rare gas atom projected onto the surface. The interactions between the four moving Pt atoms and the remainder of the Pt surface were mimicked with an effective GLE. The friction kernel for the GLE was selected to reproduce vibrational properties of the Pt(111) surface.<sup>23</sup> The Pt(111) surface in the model was rather smooth, with only a 0.1 kJ/mol barrier to surface diffusion for either Ar or Xe. The binding energy of Ar with the surface in the simulation was 9.2 kJ/mol, and that of Xe was 29.3 kJ/mol. These energies were chosen to fit experimental results.<sup>24,25</sup> There was no barrier to adsorption in this model.

In the simulation results, the sticking probability was a monotonically decreasing function of the incident energy of the atoms.<sup>1</sup> For this reason, we assume here that the energy-diffusion regime is sufficient to describe  $P_{\text{stick}}$  and  $\bar{\epsilon}$ . Thus the only parameter required for a theoretical description of  $P_{\text{stick}}$  and its energy dependence is the energy loss  $\delta$  for each of the two atoms over the range of temperatures 50–2000 K. We assume that  $\delta$  can be written as  $\Delta E/k_B T$  where  $\Delta E$  has no temperature dependence. In terms of a GLE, this is equivalent to the harmonic bath requirement that the friction kernel  $\gamma(t)$  has no temperature dependence. We use  $\Delta E = 1.1$  kJ/mol for Ar and  $\Delta E = 5.4$  kJ/mol for Xe. The fits are noticeably worse for changes in  $\Delta E$  larger than 0.2 kJ/mol.

In the top panel of Fig. 1 we depict  $P_{\text{stick}}$  for Ar and Xe atoms on a Pt(111) surface. In the simulations the atoms were monoenergetic with total translational energy  $E_0$  and a  $\cos \theta$  angular distribution with respect to the surface normal. Assuming that  $P_{\text{stick}}$  depends only the translational energy of the atom normal to the surface, we estimate the sticking probability as

$$P_{\text{stick}} = \int_0^{\pi/2} d\theta \cos \theta \kappa(E_0 \cos^2 \theta / k_B T_S). \quad (42)$$

The surface temperature  $T_S$  in the simulations was 250 K. The normal energy scaling we assume in our theoretical analysis is not entirely correct because the Pt(111) surface is not flat. Indeed,  $P_{\text{stick}}$  the simulations did not obey normal energy scaling, i.e., the sticking probability was not exclusively dependent on the incident translational energy in the direction normal to the surface.<sup>1</sup> The corrugation of the sur-

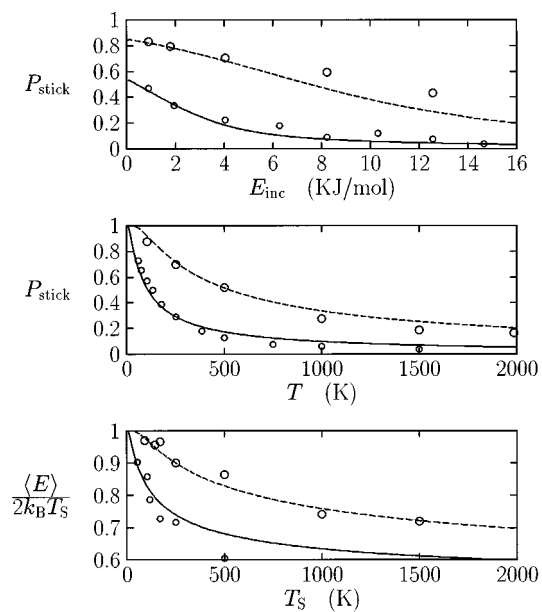


FIG. 1. Top: Energy dependence of the sticking probability for Ar (small circles) and Xe (large circles) on Pt(111) at a surface temperature of 250 K. Incident atoms are monoenergetic with a  $\cos \theta$  angular distribution. Middle: Temperature dependence of sticking probability for Ar (small circles) and Xe (large circles). The surface is at temperature  $T$ ; the incident gas is Maxwell-Boltzmann at temperature  $T$ , with a  $\cos \theta$  angular distribution. Bottom: Mean translational energy of thermally desorbing Ar (small circles) and Xe (large circles), in units of  $2k_B T_S$ , where  $T_S$  is the temperature of the surface. Solid lines are theoretical fits for Ar; dashed lines are for Xe. The simulation results are from Ref. 1.

face allowed for energy transfer between the normal directions and directions parallel to the surface. In spite of the deviations from normal energy scaling, however, the fit we present for Ar is very good. The fit for Xe underestimates  $P_{\text{stick}}$  for larger energies. This is due in large part to the theoretical assumption that the energy loss  $\delta$  is independent of the energy of the incident atom. In reality, the energy loss increases with increasing incident energy. A larger energy loss results in a larger sticking probability in the energy diffusion regime. This effect will be discussed in greater detail in Sec. III B 2.

The middle panel of Fig. 1 shows the sticking probability for a thermal distribution of atoms incident on a Pt(111) surface of the same temperature. The theoretical fits again provide excellent agreement with the simulation results over a wide range of temperatures. The small differences between the simulation results and the theoretical fits can be ascribed to two sources. First, the energy loss  $\Delta E$  has some energy dependence because the Pt(111) surface is anharmonic. Second, the multidimensional nature of the reaction coordinate is neglected in the theoretical fit.

In the bottom panel of Fig. 1 the average energy of escaping particles is shown relative to  $2k_B T_S$ , where  $T_S$  is the temperature of the surface. Because there is no barrier to adsorption,  $E$  is the total translational energy of a desorbed particle far from the surface. According to transition state theory,  $\langle E \rangle = 2 k_B T_S$ : each of the two translational degrees of freedom parallel to the surface has  $(1/2) k_B T_S$  of energy,

while the flux-weighted normal direction has  $1 k_B T_S$ . Again the theoretical fit performs well for both Ar and Xe. The only significant discrepancy is for Ar desorbing at 500 K. Our excellent agreement with the data overall suggests the possibility that the simulation result at this single point might be in error.

## B. Simulation tests of the interpolation formulas

In this section, we compare simulation results for escape from a metastable well  $V(q)$  to the predictions of the interpolation formulas relating the reaction coordinate  $q$  to the unstable mode  $\rho$  of PGH theory. The potential  $V(q)$  is piecewise harmonic with a metastable well,

$$V(q) = \begin{cases} \frac{1}{2}\mu\omega_0^2(q+q_0)^2, & q \leq -q^* \\ V^\ddagger - \frac{1}{2}\mu\omega^\ddagger{}^2, & q > -q^* \end{cases} \quad (43)$$

Continuity of  $V(q)$  and its derivative implies  $q_0/q^* = 1 + (\omega^\ddagger/\omega_0)^2$  and  $V^\ddagger = \frac{1}{2}\mu\omega^\ddagger{}^2 q^* q_0$ . Ohmic friction was employed,  $\gamma(t-t') = 2\gamma_0\delta(t-t')$ . Parameters were selected to give  $V^\ddagger = 5 k_B T$ ,  $\omega_0 = \omega^\ddagger = 1$ , and  $\mu = 1$ . For Ohmic friction, Eq. (30) reduces to

$$\delta = \gamma_0 \times 2\beta \int_{q_l}^0 dq \sqrt{2[V^\ddagger - V(q)]} = 33.5619 \times \gamma_0. \quad (44)$$

The above is the weak-damping expression for  $\delta$ , and  $q_l$  is the left-hand turning point at energy  $V^\ddagger$ ,  $q_l = -q_0 - \sqrt{2V^\ddagger}$ .

We performed two sets of simulations of escape from the metastable well  $V(q)$ . In the first set of simulations, we varied the static friction  $\gamma_0$  to obtain  $\bar{\epsilon}$  and  $\kappa$  as a function of the energy loss parameter  $\delta$ . Values of  $\delta$  ranged from  $10^{-2}$  to  $10^3$ . For weak to moderate friction,  $\delta < 10^{2.5}$ , 50 000 pairs of trajectories were initiated for each choice of  $\delta$ . The two trajectories of each pair started with a common initial energy chosen from the distribution  $\exp(-\epsilon)$ . One trajectory started with an initial  $\dot{q} > 0$ , and the other with  $\dot{q} < 0$ . An independent sampling of the random force  $\xi(t)$  was used for each trajectory. For large friction,  $\delta = 10^{2.5} - 10^3$ ,  $\kappa(\epsilon)$  was sampled at discrete values of the energy  $\epsilon$  and  $\bar{\epsilon}$  was obtained by integration. At  $\delta = 10^{2.5}$ , 20 000 pairs of trajectories were initiated at the values  $\epsilon = 0.25, 0.5, \dots, 8$  to compute  $\kappa(\epsilon)$ . For  $\delta = 10^{2.75}$ , 5000 pairs of trajectories were initiated at  $\epsilon = 0.25, 0.5, \dots, 8$ . For the largest friction,  $\delta = 10^3$ , between 15 000 and 125 000 pairs of trajectories were initiated at energies ranging from  $\epsilon = 0.05$  to  $\epsilon = 10$ . In all of these simulations except for  $\delta = 10^3$ , trajectories of escaping particles were terminated when the energy of the particle fell below the minimum of the metastable well. For  $\delta = 10^3$ , trajectories of all particles were terminated when the energy was less than  $1 k_B T$  above the minimum.

In the second set of simulations, we varied the initial energy  $\epsilon$  to obtain  $\kappa(\epsilon)$  for four choices of  $\delta$ ,  $\delta = 10^{-0.5}, 10^{0.5}, 10^{1.5}$ , and  $10^2$ . We ran 40 000 trajectories for each choice of  $\delta$  and  $\epsilon$ , half with initial  $\dot{q} < 0$  and half with  $\dot{q} > 0$ .

### 1. The average energy of escaping particles $\bar{\epsilon}$

In Fig. 2 we display results obtained for  $\bar{\epsilon}$  for escape from  $V(q)$ . The solid line in Fig. 2 is calculated using Eq.

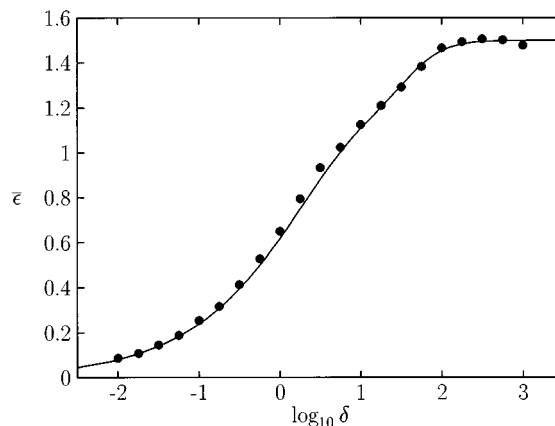


FIG. 2. The average energy of escaping particles relative to the barrier-top energy in units of  $k_B T$  is shown as a function of the damping parameter  $\delta$ . Points are reactive flux simulations; the line is the interpolation formula, Eq. (40). Statistical uncertainties in the simulation results are smaller than the size of the points.

(40). It is evident that the interpolation formula provides an accurate estimate of the energies of escaping particles for the entire damping range. The results show that particles escape from the well with very little energy when the damping is small. The energy of escaping particles attains the transition state value of  $1 k_B T$  for moderate friction,  $1 < \delta < 10$ . For larger friction,  $\bar{\epsilon}$  saturates at the predicted value of  $(3/2) k_B T$ .

We now describe the behavior in each of these regions in greater detail. At small damping,  $\delta \leq 10^{-0.5}$ , the agreement between the theoretical expression and the simulation results is virtually exact. The reaction coordinate  $q$  is essentially the same as the unstable barrier normal mode  $\rho$ , and the energy loss  $\delta$  for the unstable normal mode is given very accurately by the lowest order perturbation theory, Eq. (30). Frictional recrossings are not important, and the particle escapes as soon as sufficient energy has diffused into the reaction coordinate to allow escape over the barrier.

In the moderate friction regime, energy exchange between the particle and the frictional bath is sufficiently rapid that the equilibrium distribution of energies is maintained even at the barrier top. The Grote-Hynes factor, measuring frictional recrossings, ranges from 0.99 at  $\delta = 1$  to 0.86 at  $\delta = 10$ , indicating that frictional recrossings are relatively unimportant and that transition state theory estimate for  $\bar{\epsilon}$  should be accurate. Consequently the average energy of escaping particles is close to the transition state theory estimate of  $1 k_B T$ . Although the agreement between theory and simulation is generally good in this region, the theoretical prediction for  $\bar{\epsilon}$  is systematically smaller than the simulation results. As will be discussed in greater detail in Sec. III B 2 on  $\kappa(\epsilon)$ , the theory underestimates  $\kappa(\epsilon)$  for large energies and overestimates  $\kappa(\epsilon)$  for small energies. These small errors accumulate to produce a value for  $\bar{\epsilon}$  that is smaller than the value obtained in simulations.

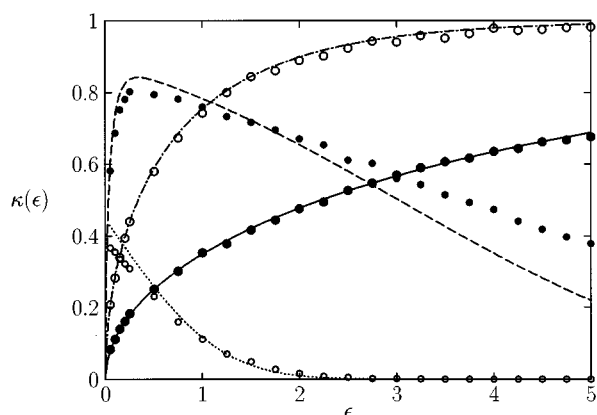


FIG. 3. The energy-dependent transmission coefficient  $\kappa(\epsilon)$  is shown as a function of the damping parameter  $\delta$ . Points are results of reactive flux simulations; lines are the interpolation formula, Eq. (41). The dotted line and small open circles are weak friction ( $\delta=10^{-0.5}$ ); the dashed line and small filled circles are moderate friction ( $\delta=10^{0.5}$ ); the dot-dashed line and large open circles are strong friction ( $\delta=10^{1.5}$ ); the solid line and large filled circles are the strongest friction ( $\delta=10^2$ ).

When the frictional damping is large,  $\delta \geq 10^{1.5}$ , the agreement between the interpolation formula and the simulation results is again very good. Only dynamics near the barrier top is important when the frictional damping is large, and the parabolic barrier expression, Eq. (24), provides an excellent estimate for  $\bar{\epsilon}$ . The simulation results approach the theoretical plateau value of  $\bar{\epsilon} = (3/2)k_B T$ . The last simulation point,  $\delta = 10^3$ , gives an energy which falls slightly below  $(3/2)k_B T$ . The error bars for this point are roughly the size of the point itself. It is likely that the difference between the prediction and the simulation result is due to statistical noise in the simulation. The transmission coefficient for  $\delta = 10^3$  is very small,  $\kappa = 0.034$ , making statistics difficult to collect.

## 2. The energy dependent transmission coefficient $\kappa(\epsilon)$

To examine the energy distribution of escaping particles in more detail, and to test the underlying assumptions of PGH theory, we have used simulations to obtain the energy-dependent transmission coefficient  $\kappa(\epsilon)$  defined by Eq. (8). The results of simulations are shown as points in Fig. 3, and theoretical predictions are shown as lines. Data are presented for four values of the energy loss  $\delta$ : weak damping,  $\delta = 10^{-0.5}$ ; moderate damping,  $\delta = 10^{0.5}$ ; strong damping,  $\delta = 10^{1.5}$ ; and very strong damping,  $\delta = 10^2$ .

The general shape of the curves, a rise to a maximum and then a gradual decline, demonstrates the interplay between energy diffusion in the weak damping limit and frictional recrossings in the strong friction limit. For weak friction,  $\delta = 10^{-0.5}$ ,  $\kappa(\epsilon)$  rises rapidly to its maximum value and then falls off with an exponential decay. Particles escape the well as soon as there is sufficient energy to cross the barrier, but the slow rate of energy diffusion into the reaction coordinate depletes the population of states near the barrier. In terms of a sticking probability, particles injected into the well with energy much larger than  $\delta$  bounce out without having a chance to thermalize. The energy-dependent transmission co-

efficient  $\kappa(\epsilon)$  again rises rapidly for moderate friction,  $\delta = 10^{0.5}$ , and decays slowly for higher energies. Energy diffusion is sufficiently rapid to maintain a distribution of energies close to the equilibrium distribution. The moderate friction results are closest to transition state theory, which predicts that  $\kappa(\epsilon) = 1$  for all  $\epsilon > 0$ . When the frictional damping becomes larger, the rise of  $\kappa(\epsilon)$  becomes slower. This is seen in the strong friction results,  $\delta = 10^{1.5}$ . Particles with small energies are buffeted by frictional forces at the barrier and  $\kappa(\epsilon)$  is small. The same behavior is seen at the largest friction,  $\delta = 10^2$ . For these largest two values of the damping,  $\kappa(\epsilon)$  is monotonically increasing for the range of energies depicted. Eventually, when  $\epsilon$  is sufficiently large, these two curves will also reach a maximum and then decrease so as to resemble the general form of  $\kappa(\epsilon)$  for smaller values of the damping.

The details of the theoretical curves in relation to the simulation results reveal minor shortcomings in the theoretical assumptions. We begin with an examination of the results for the smallest friction in Fig. 3,  $\delta = 10^{-0.5}$ . The theoretical curve is the product  $\kappa_{\text{pb}}(\epsilon)\kappa_{\rho}(\epsilon)$ . Since the Grote-Hynes factor  $\kappa_{\text{pb}}(\epsilon)$  rises rapidly from its initial value of 0 at  $\epsilon = 0$  to its asymptotic value of 1 [ $\kappa_{\text{pb}}(\epsilon) = 0.99$  by the time that  $\epsilon = 0.03 k_B T$ ],  $\kappa(\epsilon) \approx \kappa_{\rho}(\epsilon)$  for weak damping. It is evident here that the theoretical results overestimate  $\kappa(\epsilon)$  for smaller energies. One explanation for this systematic error is that the theoretical estimate for the energy loss  $\delta$  is too large: a larger value for  $\delta$  results in faster energy transfer between the particle and the bath and a larger reaction rate in the low friction regime. The theoretical prediction for  $\delta$  might indeed be too large because it is taken from the lowest order of a perturbation theory ordered by the frictional damping  $\gamma(t)$  and by the inverse of the barrier height  $1/\beta V^{\ddagger}$ . The next contribution to the energy loss is expected to reduce the magnitude of the effective energy loss by roughly a factor  $1/\beta V^{\ddagger}$ .<sup>19</sup> Since a smaller energy loss implies a smaller escape rate, it is reasonable that  $\kappa(\epsilon)$  obtained from simulation is smaller than that predicted by theory, especially for energies close to the barrier energy.

The theoretical prediction is also seen to be too small for  $\kappa(\epsilon)$  for small energies for intermediate friction,  $\delta = 10^{0.5}$ . For energies smaller than  $1.5 k_B T$ , the theoretical prediction is smaller than the essentially exact results from simulations. The reason, again, is that the truncated perturbation theory for  $\delta$  neglects a contribution on the order of  $1/\beta V^{\ddagger}$  which acts to decrease the size of  $\delta$ . In the intermediate friction results for energies larger than  $2 k_B T$ , however, an error in the other direction is apparent: the theoretical prediction for  $\kappa(\epsilon)$  is smaller than the simulation results. This error is again due to an error in the theoretical assumption for  $\delta$ ; in this case, the theoretical value for  $\delta$  is too small, leading to a predicted transmission coefficient which is too small. The value of  $\delta$  from the theory is too small because of the assumption that  $\delta$  is constant as a function of the energy  $\epsilon$ . The energy loss in fact depends on the energy at which the particle traverses the metastable well. When friction is very weak, the reactive flux over the barrier is very close to the barrier energy and the variations with  $\delta$  as a function of  $\epsilon$  are

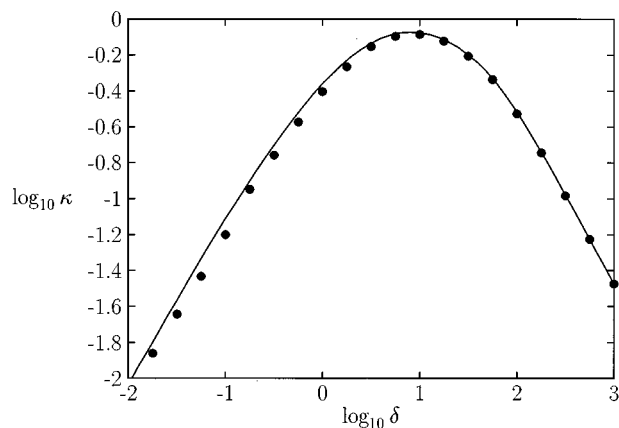


FIG. 4. The transmission coefficient  $\kappa$  is shown as a function of the damping parameter  $\delta$ . Points are results of reactive flux simulations; the line is the prediction of turnover theory, Eq. (31a)–(31d). Statistical uncertainties in the simulation results are smaller than the size of the points.

small. In the intermediate friction case, however, a broader range of energies is relevant, and the variation of  $\delta$  with  $\epsilon$  is evident in the simulation results. Indeed, the energy loss per circuit over the well should be roughly proportional to the initial energy, making  $\delta$  an increasing function of the energy. Energetic particles injected into the well lose more energy than the theory predicts, are therefore more likely to be trapped in the metastable well.

The simulation results and the theoretical estimate agree well for strong friction,  $\delta=10^{1.5}$  and  $10^2$ . The energy diffusion factor  $\kappa_\rho(\epsilon) > 0.99$  for the entire range of energies depicted, and  $\kappa(\epsilon) \approx \kappa_{\text{pb}}(\epsilon)$ . The energy diffusion factor will eventually decrease for large enough  $\epsilon$ , causing  $\kappa(\epsilon)$  to decrease and return to 0. Such high energies would not be important for thermal escape.

The results for weak to moderate friction shed light on why the estimate that  $\delta$  is independent of energy<sup>2–4</sup> can be reasonably accurate for predictions of barrier crossing rates. The theoretical approximation that  $\delta$  is a constant underestimates  $\kappa(\epsilon)$  for large  $\epsilon$ . The same approximation, along with the neglect of quantities on the order of  $1/\beta V^{\ddagger}$ , overestimates  $\kappa(\epsilon)$  for small  $\epsilon$ . These errors are in compensating directions, yielding a net result for the transmission coefficient  $\kappa$  which agrees well with simulation results. At the smallest values of the energy loss  $\delta$ , the simulations described here reveal a small but systematic error made by the theory in predicting a  $\kappa$  slightly larger than the value obtained by simulations. Simulation results for  $\kappa$  are shown as points in Fig. 4, and the theoretical estimate, Eqs. (31a)–(31d), is depicted as the solid line. For  $\delta \leq 10^{-0.5}$ , the theoretical prediction is too large by a factor of about 20%. This difference is of the same magnitude as  $1/\beta V^{\ddagger} = 1/5$  in the simulations.

### 3. The normalized energy distribution of escaping particles $f(\epsilon)$

The normalized distribution of energies of escaping particles,  $\exp(-\epsilon)\kappa(\epsilon)/\kappa$ , is displayed in Fig. 5. As before, small open circles are weak friction ( $\delta=10^{-0.5}$ ); small filled

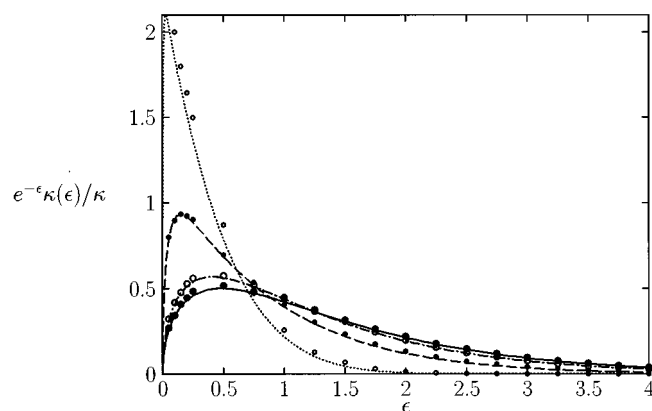


FIG. 5. The normalized distribution of energies of escaping particles,  $e^{-\epsilon}\kappa(\epsilon)/\kappa$ , is shown as a function of the reduced energy  $\epsilon$  for various choices of the damping parameter  $\delta$ . Points are results of reactive flux simulations; lines use the interpolation formula, Eq. (41), for  $\kappa(\epsilon)$ , and  $\kappa = \kappa_{\text{pb}}\kappa_\rho$ . The dotted line and small open circles are  $\delta=10^{-0.5}$ ; the dashed line and small filled circles are  $\delta=10^{0.5}$ ; the dot-dashed line and large open circles are  $\delta=10^{1.5}$ ; the solid line and large filled circles are  $\delta=10^2$ .

circles are moderate friction ( $\delta=10^{0.5}$ ); large open circles are strong friction ( $\delta=10^{1.5}$ ); and large filled circles are the strongest friction ( $\delta=10^2$ ). The lines correspond to the theoretical estimate  $\exp(-\epsilon)\kappa_{\text{pb}}(\epsilon)\kappa_\rho(\epsilon)/\kappa$ , where  $\kappa = \kappa_{\text{pb}}\kappa_\rho$ .

There is a small but noticeable difference between the simulation results and the theoretical estimate for the smallest value of the damping,  $\delta=10^{-0.5}$ . The theory predicts a distribution  $f(\epsilon)$  shifted to lower energies than the distribution obtained by simulations. It is likely that the theoretical assumption that  $\delta$  is a constant independent of  $\epsilon$  is responsible for the shift of the theoretical prediction to lower energies. More energetic particles will have an effective  $\delta$  which increases with  $\epsilon$ , and will have a larger probability to remain trapped in the well than predicted using the assumption that  $\delta$  is constant. The difference between the theoretical prediction and the simulation results is virtually undetectable for moderate friction,  $\delta=10^{0.5}$ . For strong friction,  $\delta \geq 10^{1.5}$ , the normalized distribution of energies of escaping particles is seen to approach the limiting form  $2 \exp(-\epsilon)\sqrt{\epsilon/\pi}$ .

### C. Optimal sampling for reactive flux simulations

The energy-dependent transmission coefficient  $\kappa(\epsilon)$  can be used to characterize the relative efficiencies of various methods for selecting initial conditions for reactive flux calculations of reaction rates. The energy-dependent transmission coefficient  $\kappa(\epsilon)$  can also be used to design an optimally efficient reactive flux sampling scheme, one that converges  $\kappa$  with the least amount of computational effort. Although this optimal sampling analysis relies on knowledge of  $\kappa(\epsilon)$ , which implies that  $\kappa$  itself is known, it can serve as a guide when  $\kappa(\epsilon)$  can be estimated.

Instead of restricting attention to GLE dynamics, let us suppose that the system of interest has a Hamiltonian  $H$ . A reaction coordinate  $q$  is singled out from the coordinates and  $p$  is the momentum conjugate to  $q$ . The momentum is assumed to appear in  $H$  as the kinetic energy term  $p^2/2\mu$ ,

where  $\mu$  is a reduced mass. The energy  $\epsilon$  is defined as  $\beta p^2/2\mu$ . The rate constant corresponding to transitions from reactant ( $q < q^\ddagger$ ) to product ( $q > q^\ddagger$ ) is  $\kappa k_{\text{tst}}$ . The transition state theory rate constant  $k_{\text{tst}}$  is

$$k_{\text{tst}} = \frac{\langle \delta(q - q^\ddagger) |\dot{q}| \Theta[\dot{q}] \rangle}{\langle \Theta(q^\ddagger - q) \rangle} \quad (45)$$

and the transmission coefficient is

$$\kappa = \frac{\langle \delta(q - q^\ddagger) |\dot{q}| \Theta[\dot{q}] \Theta[q(\tau)] \rangle - \langle \delta(q - q^\ddagger) |\dot{q}| \Theta[-\dot{q}] \Theta[q(\tau)] \rangle}{\langle \delta(q - q^\ddagger) |\dot{q}| \Theta[\dot{q}] \rangle}. \quad (46)$$

Starting at time 0 from  $q^\ddagger$  with velocity  $\dot{q}$ , the position of the reaction coordinate after a plateau time  $\tau$  is  $q(\tau)$ . As usual,  $\Theta[\dots]$  is the Heaviside function.

The transmission coefficient can be obtained through simulations by selecting  $M$  pairs of initial coordinates and momenta from a probability distribution proportional to  $\exp[-\beta H] \delta(q - q^\ddagger) \Theta[\dot{q}] \Phi(\dot{q})$ , running a pair of trajectories with initial reaction coordinate velocities  $\pm \dot{q}$  for each choice, and estimating  $\kappa$  from the cumulative average  $\kappa_M$ ,

$$\kappa_M = \frac{\sum_{m=1}^M W(\dot{q}) \{ \Theta[q(\tau; \dot{q})] - \Theta[q(\tau; -\dot{q})] \}}{\sum_{m=1}^M W(\dot{q})}. \quad (47)$$

The sampling function  $\Phi(\dot{q})$  and the weighting function  $W(\dot{q})$  have the relationship  $\Phi(\dot{q})W(\dot{q}) = |\dot{q}|$ . The introduction of  $\Phi(\dot{q})$  and  $W(\dot{q})$  serves as a type of nonequilibrium sampling.<sup>26-29</sup> Whereas nonequilibrium sampling is usually designed to enhance the sampling of the coordinates, this type of nonequilibrium sampling is designed to enhance the sampling of velocities.

The Maxwellian velocity distribution corresponds to the choice  $\Phi(\dot{q}) = 1$  and  $W(\dot{q}) = |\dot{q}|$ . Another common choice is the Maxwellian flux distribution, which has  $\Phi(\dot{q}) = |\dot{q}|$  and  $W(\dot{q}) = 1$ . The Maxwellian flux distribution shifts the selection of the reaction coordinate kinetic energy to slightly higher energies than the pure Maxwellian distribution. We will show that the Maxwellian distribution performs better than the Maxwellian flux when the frictional damping is weak and less energetic particles contribute to the reactive flux. For strong damping, more energetic particles contribute to the reactive flux, and the Maxwellian flux distribution performs better than the pure Maxwellian distribution.

Instead of describing the initial conditions in terms of the velocity  $\dot{q}$ , we choose to make contact with our expressions for  $\kappa(\epsilon)$  and describe the initial conditions in terms of the reduced energy  $\epsilon$ . Rather than selecting a reaction coordinate velocity from the distribution  $\exp(-\beta\mu\dot{q}^2/2)\Phi(\dot{q})$  (where we recall that the exponential arises from the factor  $e^{-\beta H}$ ), we select an energy  $\epsilon$  from a distribution  $\phi(\epsilon)$ . The relationship between these two distributions is  $\phi(\epsilon)d\epsilon \propto \exp(-\beta\mu\dot{q}^2/2)\Phi(\dot{q})|\dot{q}|d\dot{q}$ . The kinetic energy must be non-negative classically, implying that  $\phi(\epsilon) = 0$  for  $\epsilon < 0$ . For positive energies,  $\phi(\epsilon) > 0$  because it is a probability distribution. The normalization of  $\phi(\epsilon)$  is

$$\int_0^\infty d\epsilon \phi(\epsilon) = 1. \quad (48)$$

The weighting function corresponding to  $\phi(\epsilon)$  is termed  $w(\epsilon)$  and is defined by the relationship

$$\phi(\epsilon)w(\epsilon) = \exp(-\epsilon). \quad (49)$$

The Maxwellian distribution corresponds to  $\phi(\epsilon) = \exp(-\epsilon)/\sqrt{\pi\epsilon}$ , and the Maxwellian flux distribution corresponds to  $\phi(\epsilon) = \exp(-\epsilon)$ . Since the average value of  $w(\epsilon)$  over the distribution  $\phi(\epsilon)$  is unity, the transmission coefficient from Eq. (47) can be written as

$$\kappa_M = \frac{1}{M} \sum_{m=1}^M w(\epsilon_m) \{ \theta^+(\epsilon_m) - \theta^-(\epsilon_m) \}, \quad (50)$$

where  $\theta^\pm(\epsilon) = \Theta[q(\tau; \pm \sqrt{2\epsilon k_B T/\mu}) - q^\ddagger]$ .

For each trajectory in the  $M$  pairs, the initial coordinates and momenta (other than the momentum  $p$  of the reaction coordinate) are chosen from the distribution  $\exp[-\beta(V+T)]\delta(q - q^\ddagger)$ , while the kinetic energy  $\epsilon$  of the reaction coordinate is drawn from the distribution  $\phi(\epsilon)$ .

In order that the two trajectories of the  $m$ th pair be uncorrelated, we will assume that the coordinates and momenta, other than  $p$ , are chosen independently. This corresponds to using independent samplings of the stochastic force  $\xi(t)$  in a GLE simulation. Using the same initial coordinates and momenta for both trajectories in the  $m$ th pair would decrease the sampling efficiency by introducing correlation between the two trajectories of the  $m$ th pair. To illustrate this point, suppose that signs of the initial coordinates and momenta for the trajectory contributing to  $\theta^+(\epsilon_m)$  are reversed to obtain the initial conditions for the trajectory contributing to  $\theta^-(\epsilon_m)$ . If the potential energy surface is symmetric with respect to inversion, then symmetry requires  $\theta^-(\epsilon_m) = 1 - \theta^+(\epsilon_m)$ , and  $\theta^+(\epsilon_m)$  and  $\theta^-(\epsilon_m)$  are perfectly correlated.

Returning to Eq. (50), the quantity being averaged,  $w(\epsilon)[\theta^+(\epsilon) - \theta^-(\epsilon)]$ , possesses an intrinsic variance  $\sigma_\kappa^2$  which depends on the choice of  $\phi(\epsilon)$ . This variance is defined as

$$\sigma_\kappa^2 = \int_0^\infty d\epsilon \phi(\epsilon)w^2(\epsilon) \langle [\theta^+(\epsilon) - \theta^-(\epsilon)]^2 \rangle \quad (51)$$

$$- \left\{ \int_0^\infty d\epsilon \phi(\epsilon)w(\epsilon) \langle \theta^+(\epsilon) - \theta^-(\epsilon) \rangle \right\}^2. \quad (52)$$

The angle brackets imply an average over the distribution  $\exp(-\beta H)\exp(\epsilon)\delta(q - q^\ddagger)$ . Since the  $M$  pairs of trajectories are uncorrelated, the statistical uncertainty of the cumulative

TABLE I. The mean square error  $\sigma_\kappa^2$  expected for reactive flux sampling of the transmission coefficient is shown for various sampling distributions in the weak friction and strong friction limits.

Distribution $\phi(\epsilon)$	$\sigma_\kappa^2$ to leading order	
	Weak friction, $\delta \ll 1$	Strong friction
Maxwellian <sup>a</sup>	$\frac{1}{2}\pi\kappa\sqrt{\bar{\epsilon}} \sim \delta^{1.25}$	$\pi/4$
Maxwellian flux <sup>b</sup>	$\frac{\kappa}{1+\bar{\epsilon}} \sim \delta$	$1/2$
Optimal <sup>c</sup>	$\frac{\kappa\bar{\epsilon}}{(1/2+\bar{\epsilon})^2} \sim \delta^{1.5}$	$1/2$

<sup>a</sup> $\phi(\epsilon) = \exp(-\epsilon)/\sqrt{\pi\epsilon}$ .

<sup>b</sup> $\phi(\epsilon) = \exp(-\epsilon)$ .

<sup>c</sup> $\phi(\epsilon)$  given by Eq. (B4).

average  $\kappa_M$  is  $\sqrt{\sigma_\kappa^2/M}$ . The optimal choice for  $\phi(\epsilon)$  is the probability distribution which minimizes  $\sigma_\kappa^2$  and thereby produces the cumulative average with the smallest statistical fluctuations. We derive expressions for the optimal  $\phi(\epsilon)$  in Appendix II.

In Table I,  $\sigma_\kappa^2$  is shown for three distributions: the Maxwellian distribution, the Maxwellian flux distribution, and the optimal distribution. Results are shown for both strong friction and weak friction, assuming in each case that  $\kappa \ll 1$ . Limiting forms of  $\kappa(\epsilon)$ ,

$$\begin{aligned} \kappa(\epsilon) &\approx 2\kappa\sqrt{\epsilon/\pi}, & \text{moderate to strong damping;} \\ \kappa(\epsilon) &\approx (\kappa/\bar{\epsilon})\exp(-\epsilon/\bar{\epsilon}), & \text{weak damping,} \end{aligned} \quad (53)$$

were used in the calculation of  $\phi(\epsilon)$  and  $\sigma_\kappa^2$  for the optimal distribution.

For weak friction,  $\bar{\epsilon} \approx 0.82\delta$ .<sup>2</sup> The optimal distribution for weak friction is  $\phi(\epsilon) = (1/2\bar{\epsilon})\exp(-\epsilon/2\bar{\epsilon})$ , producing  $\sigma_\kappa^2 = \kappa\bar{\epsilon}/(1/2+\bar{\epsilon})^2$ . In the weak friction limit, the energy loss  $\delta \ll 1$ , and  $\sigma_\kappa^2 \propto \delta^{3/2}$  for the optimal sampling distribution. The relative error for a simulation is proportional to  $\sqrt{\sigma_\kappa^2}/\kappa$ . For weak friction,  $\kappa \approx \delta$ , and the relative error  $\propto \delta^{-1/4}$  for the optimal distribution. The Maxwellian distribution  $\exp(-\epsilon)/\sqrt{\pi\epsilon}$ , produces  $\sigma_\kappa^2 \propto \delta^{5/4}$  and a relative error  $\propto \delta^{-3/8}$ , slightly worse than the optimal distribution. Of the three distributions, the Maxwellian flux distribution is weighted toward the highest energies and produces the largest variance,  $\sigma_\kappa^2 \propto \kappa/(1+\bar{\epsilon}) \propto \delta$ . The relative error of the Maxwellian flux distribution is also the largest, scaling as  $\delta^{-1/2}$ . In terms of the relative error, the sampling from the optimal distribution is more efficient than sampling from the Maxwellian flux distribution by a factor of  $\delta^{-1/4}$ . When  $\delta=0.01$ , e.g., this corresponds to a factor of 3 enhancement of the computational efficiency when the optimal distribution is used instead of the Maxwellian flux distribution.

For moderate to strong friction, the differences between the sampling efficiencies for the three choices of  $\phi(\epsilon)$  are less substantial. In this case the optimal distribution is the same as the Maxwellian flux distribution to leading order in  $\kappa$ , and both the optimal distribution and the Maxwellian flux distribution produce  $\sigma_\kappa^2 = 1/2$  to leading order. The Maxwellian distribution performs slightly worse, giving  $\sigma_\kappa^2 = \pi/4$  to leading order in  $\kappa$ . All three distributions produce roughly

the same variance in the strong damping limit because each decays as  $\exp(-\epsilon)$ . Although the Maxwellian distribution is singular,  $\sim \epsilon^{-1/2}$  as  $\epsilon \rightarrow 0$ , this is an integrable singularity which produces little change in the overall sampling efficiency.

When friction is strong, the relative error scales as  $1/\kappa$  for each of the three distributions. Thus for a fixed number  $M$  of trajectories, the statistical uncertainty in the measured  $\kappa$  increases rapidly with decreasing  $\kappa$ . Since the error after  $M$  trajectories scales as  $1/\sqrt{M}$ , the number of trajectories must be on the order of  $1/\kappa^2$  before the relative error is of order unity.

We note that there are other methods of enhancing the sampling efficiency of reactive flux simulations. One could, for instance, sample  $\kappa(\epsilon)$  directly for discrete choices of  $\epsilon$ . Calling the  $i$ th choice  $\epsilon_i$ , the transmission coefficient  $\kappa_i$  for particles with initial kinetic energy  $\epsilon_i$  can be calculated from reactive flux simulations. The total transmission coefficient  $\kappa$  can be obtained by a quadrature of the discrete points  $e^{-\epsilon_i}\kappa_i$ . Indeed, this was our method for obtaining  $\bar{\epsilon}$  in the large damping regime. A slightly more elaborate treatment would be to partition the sampling of initial reaction coordinate kinetic energies into bins, to calculate  $\exp(-\epsilon)\kappa(\epsilon)$  within each bin, and to sum the result to give the total  $\kappa$ . If friction is low, it is efficient to concentrate sampling on the bins with small initial energies. For large friction, bins with larger initial energies contribute more strongly to  $\kappa$ .

The absorbing boundary method has also been shown to be quite efficient for reactive flux simulations.<sup>30,31</sup> This method is formally not exact—it does not produce the exact value for  $\kappa$  as the number of trajectories  $M \rightarrow \infty$ —but it has been shown to be an excellent approximation in practice. With this method, trajectories are terminated if they return to the transition state dividing surface, and a statistical approximation is used to relate the decay of the population to the transmission coefficient.

## IV. CONCLUSIONS

In comparing our simulation results for escape over a barrier in a one-dimensional GLE with theoretical predictions, we found good agreement when the frictional damping of the reaction coordinate was large. For weak to moderate damping, we detected systematic errors in the predictions of the analytic theory. These errors are relevant to the PGH turnover theory for reaction rates.<sup>2,3</sup> When the energy  $\epsilon$  of an escaping particle is just above the barrier energy, the theoretical prediction for  $\kappa(\epsilon)$  is too large. Conversely, when the particle has an energy much larger than the barrier energy, the predicted value of  $\kappa(\epsilon)$  is too small. These errors can be understood in light of two of the assumptions of PGH theory: first, that the lowest order of perturbation theory in the inverse barrier height  $1/\beta V^\ddagger$  is sufficient to obtain  $\delta$ ; second, that the energy loss  $\delta$  is independent of the energy  $\epsilon$ . The first assumption results in a value for  $\delta$  that is too large overall by a factor of roughly  $[1 - (\beta V^\ddagger)^{-1}]$ .<sup>19</sup> This causes  $\kappa(\epsilon)$  to be too large by the same factor for energies close to the barrier energy. Furthermore, the theoretical prediction for  $\kappa$  is also too large by a factor of roughly  $[1 - (\beta V^\ddagger)^{-1}]$ . The

second assumption of a constant energy loss  $\delta$  underestimates the energy loss for energetic particles and predicts too small a value for  $\kappa(\epsilon)$ . These errors combine to skew predictions for the energy distribution of escaping particles to slightly lower energies than are observed in simulations. When the transmission coefficient itself is considered, however, these errors are in compensating directions. This cancellation of errors works to the favor of the PGH turnover theory.

We have applied the theoretical expressions for weak friction to describe simulations of Ar and Xe interacting with the Pt(111) surface.<sup>1</sup> Our expressions provide adequate single parameter fits for simulation results for sticking probabilities of atoms in a monoenergetic beam and for atoms from a thermal distribution incident on the Pt surface. Good fits are also obtained for the average energy of atoms desorbing thermally from the surface. Our analysis could be extended easily to describe the accommodation coefficient, which measures the energy transfer between incident particles and a surface.<sup>32-35</sup> The favorable results we obtain for atom-surface sticking are encouraging for the prospect of describing molecule-surface energy transfer and sticking probabilities with a similar approach (for a review of theoretical methods see Ref. 36).

Our expression for  $P_{\text{stick}}$  includes the possibility of multiple oscillations of the gas particle before it sticks to the surface or bounces away from the surface. It would be interesting to compare our predictions to those of prompt sticking, where it is assumed that the fate of a particle is decided after a single round-trip. Using prompt sticking expressions, others have been able to fit experimental sticking probabilities for Ne, Ar, Kr, and Xe on Ru(001).<sup>37</sup> These workers found that a quantum-mechanical treatment was necessary to describe the sticking of Ne and Ar. It would be straightforward to include a quantum description of the particle and bath using a semiclassical version of PGH turnover theory.<sup>38</sup>

The success in describing gas-surface sticking over a broad range of temperatures with a single parameter provides evidence that the expressions developed here for a one-dimensional reaction coordinate can have general validity for multidimensional systems. One such area where our approach might prove useful is in gauging the prospects of bond-selective chemistry.<sup>39-41</sup> The expressions we present for  $\kappa(\epsilon)$  could be used to estimate the probability that a molecule prepared in a high-energy reactive state will successfully traverse a barrier separating reactants from products.

## ACKNOWLEDGMENT

This work was supported by a grant from the NSF (NSF CHE-91-22-506).

## APPENDIX A: PROPERTIES OF $\Delta(S)$

Here we investigate the behavior of  $\Delta(s) = s^2 + s\tilde{\gamma}(s) - \omega^{\ddagger 2}$  near the largest positive root  $\lambda^{\ddagger}$ . We assume that  $\tilde{\gamma}(t)$  is analytic for real  $t$  and that  $\tilde{\gamma}(0)$  exists. There must be at least one positive root to the equation  $\Delta(s) = 0$  because the sign of  $\Delta(s)$  changes from negative to positive along the positive real axis: at  $s=0$ ,  $\Delta(0) = -\omega^{\ddagger 2}$ ; as

$s \rightarrow \infty$ ,  $\Delta(s)$  approaches  $s^2 + \gamma(0) - \omega^{\ddagger 2}$ , which is positive for sufficiently large  $s$ . The largest positive root of  $\Delta(s) = 0$  is termed  $\lambda^{\ddagger}$ , and we assume that it is an isolated root. Then  $\Delta(s)$  has the form  $(s - \lambda^{\ddagger})\Delta'(s)$ . Since  $\lambda^{\ddagger}$  is the largest root,  $\Delta'(s)$  must be nonzero for  $s \geq \lambda^{\ddagger}$ . Furthermore, both  $\Delta(s)$  and  $(s - \lambda^{\ddagger})$  are positive as  $s \rightarrow \infty$ , so  $\Delta'(s)$  must also be positive in this limit. Since  $\Delta'(s)$  does not change sign for  $s \geq \lambda^{\ddagger}$ ,  $\Delta'(\lambda^{\ddagger})$  is also positive. Finally, the limit of  $[(s - \lambda^{\ddagger})/\Delta(s)]$  as  $s \rightarrow \lambda^{\ddagger}$  is simply  $1/\Delta'(\lambda^{\ddagger})$ , a positive quantity.

## APPENDIX B: DERIVATION OF THE DISTRIBUTIONS FOR OPTIMAL SAMPLING

To choose the optimal form for  $\phi(\epsilon)$ , the variance defined by Eq. (52) must be minimized with respect to  $\phi(\epsilon)$ . In other words,  $\phi(\epsilon)$  is the solution to the functional derivative equation  $\delta I[\phi]/\delta\phi(\epsilon) = 0$ , where

$$I[\phi] = \alpha \left[ -1 + \int_0^\infty d\epsilon \phi(\epsilon) \right] + \int_0^\infty d\epsilon \phi(\epsilon) w^2(\epsilon) \times \langle [\theta^+(\epsilon) - \theta^-(\epsilon)]^2 \rangle, \quad (\text{B1})$$

and the constant  $\alpha$  is a Lagrange multiplier chosen to satisfy the normalization constraint, Eq. (48). Since  $w(\epsilon) = \exp(-\epsilon)/\phi(\epsilon)$ , the functional derivative is

$$\frac{\delta I[\phi]}{\delta\phi(\epsilon)} = \alpha - \exp(-2\epsilon)\phi^{-2}(\epsilon)\langle [\theta^+(\epsilon) - \theta^-(\epsilon)]^2 \rangle = 0. \quad (\text{B2})$$

The final term in Eq. (52) need not appear in  $I[\phi]$  because  $\phi(\epsilon)w(\epsilon) = e^{-\epsilon}$  and the functional derivative of this term with respect to  $\phi(\epsilon)$  vanishes.

It is necessary to relate the mean-square value  $\langle [\theta^+(\epsilon) - \theta^-(\epsilon)]^2 \rangle$  to  $\kappa(\epsilon)$ . The form of the relationship depends on the strength of the damping. For moderate to large damping (or for a parabolic barrier),  $\theta^\pm(\epsilon)$  is  $+1$  with probability  $[1 \pm \kappa(\epsilon)]/2$  and  $0$  with probability  $[1 \mp \kappa(\epsilon)]/2$ . Thus  $[\theta^+(\epsilon) - \theta^-(\epsilon)]^2$  is  $1$  with probability  $[1 + \kappa^2(\epsilon)]/2$  and  $0$  otherwise.

For escape from a metastable well when the frictional damping is weak, a good approximation is that  $\theta^+(\epsilon)$  is always  $+1$ , and that  $\theta^-(\epsilon)$  is  $+1$  with probability  $1 - \kappa(\epsilon)$  and  $0$  otherwise. The reasoning above leads to the following estimates for  $\langle [\theta^+(\epsilon) - \theta^-(\epsilon)]^2 \rangle$ :

$$\langle [\theta^+(\epsilon) - \theta^-(\epsilon)]^2 \rangle = \begin{cases} \frac{1}{2}[1 + \kappa^2(\epsilon)], & \text{moderate to strong damping} \\ \kappa(\epsilon), & \text{weak damping} \end{cases}. \quad (\text{B3})$$

In terms of  $\kappa(\epsilon)$ , the normalized solutions to the variational equation are

$$\phi(\epsilon) = \begin{cases} \frac{\exp(-\epsilon) \sqrt{1 + \kappa^2(\epsilon)}}{\int_0^\infty d\epsilon \exp(-\epsilon) \sqrt{1 + \kappa(\epsilon)}}, & \text{moderate to strong damping} \\ \frac{\exp(-\epsilon) \sqrt{\kappa(\epsilon)}}{\int_0^\infty d\epsilon \exp(-\epsilon) \sqrt{\kappa(\epsilon)}}, & \text{weak damping} \end{cases} \quad (\text{B4})$$

We note first that when transition state theory is valid,  $\kappa(\epsilon) \approx 1$  for all  $\epsilon$ . In this case, the optimal  $\phi(\epsilon) \approx \exp(-\epsilon)$ .

<sup>1</sup>J. C. Tully, *Surf. Sci.* **111**, 461 (1981).

<sup>2</sup>V. I. Mel'nikov and S. V. Meshkov, *J. Chem. Phys.* **85**, 1018 (1986).

<sup>3</sup>E. Pollak, H. Grabert, and P. Hänggi, *J. Chem. Phys.* **91**, 4073 (1989).

<sup>4</sup>H. A. Kramers, *Physica (Utrecht)* **7**, 284 (1940).

<sup>5</sup>R. Zwanzig, *J. Stat. Phys.* **9**, 215 (1973).

<sup>6</sup>P. Hänggi, P. Talkner, and M. Borkovec, *Rev. Mod. Phys.* **62**, 251 (1990).

<sup>7</sup>T. Yamamoto, *J. Chem. Phys.* **33**, 281 (1960).

<sup>8</sup>J. C. Keck, *Adv. Chem. Phys.* **13**, 85 (1967).

<sup>9</sup>J. B. Andersen, *J. Chem. Phys.* **58**, 4684 (1973).

<sup>10</sup>C. H. Bennett, in *Algorithms for Chemical Computation*, edited by R. E. Christofferson (American Chemical Society, Washington, D.C., 1977).

<sup>11</sup>D. Chandler, *J. Chem. Phys.* **68**, 2959 (1978).

<sup>12</sup>J. A. Montgomery, Jr., D. Chandler, and B. J. Berne, *J. Chem. Phys.* **70**, 4056 (1979).

<sup>13</sup>B. J. Berne, in *Activated Barrier Crossing*, edited by G. R. Fleming and P. Hänggi (World Scientific, Singapore, 1993).

<sup>14</sup>E. Pollak, *J. Chem. Phys.* **85**, 865 (1986).

<sup>15</sup>B. J. Gertner, K. R. Wilson, and J. T. Hynes, *J. Chem. Phys.* **90**, 3537 (1989).

<sup>16</sup>S. A. Adelman and R. Muralidhar, *J. Chem. Phys.* **95**, 2752 (1991).

<sup>17</sup>R. F. Grote and J. T. Hynes, *J. Chem. Phys.* **73**, 2715 (1980).

<sup>18</sup>P. Hänggi and F. Mojtabai, *Phys. Rev. A* **26**, 1168 (1982).

<sup>19</sup>J. S. Bader, B. J. Berne, and E. Pollak, *J. Chem. Phys.* (submitted).

<sup>20</sup>QUADPACK is a FORTRAN subroutine package for the numerical computation of one-dimensional integrals. It originated from a joint project of R. Piesens, E. de Doncker-Kapenga, C. Überhuber, and D. Kahaner, and is available from netlib.att.com by anonymous ftp.

<sup>21</sup>E. Pollak, J. S. Bader, B. J. Berne, and P. Talkner, *Phys. Rev. Lett.* **70**, 3299 (1993).

<sup>22</sup>Note that there is a sign error in the corresponding equation in Ref. 2.

<sup>23</sup>J. C. Tully, *J. Chem. Phys.* **73**, 1975 (1980).

<sup>24</sup>T. Engel and R. Gomer, *J. Chem. Phys.* **52**, 5572 (1970).

<sup>25</sup>B. E. Nieuwenhuys, D. Th. Meijer, and W. M. H. Sachtler, *Phys. Status Solidi* **24**, 115 (1974).

<sup>26</sup>C. H. Bennett, *J. Comput. Phys.* **22**, 245 (1976).

<sup>27</sup>J. P. Valleau and G. M. Torrie, in *Statistical Mechanics*, edited by B. J. Berne (Plenum, New York, 1977), Vol. A, p. 169.

<sup>28</sup>D. Chandler, *Introduction to Modern Statistical Mechanics* (Oxford University, New York, 1987).

<sup>29</sup>M. P. Allen and D. J. Tildesley, *Computer Simulation of Liquids* (Oxford University, New York, 1987).

<sup>30</sup>J. E. Straub and B. J. Berne, *J. Chem. Phys.* **83**, 1138 (1985).

<sup>31</sup>J. E. Straub, D. A. Hsu, and B. J. Berne, *J. Phys. Chem.* **89**, 5188 (1985).

<sup>32</sup>F. O. Goodman and H. Y. Wachman, *Dynamics of Gas-Surface Scattering* (Academic, New York, 1976).

<sup>33</sup>S. C. Saxena and R. K. Joshi (1981).

<sup>34</sup>H. J. Kreuzer and Z. W. Gortel, in *Springer Series in Surface Science* (Springer, Berlin, 1986), Vol. 1.

<sup>35</sup>T. Brunner and W. Brenig, *Surf. Sci.* **291**, 192 (1993).

<sup>36</sup>R. B. Gerber, *Chem. Rev.* **87**, 29 (1987).

<sup>37</sup>H. Schlichting, D. Menzel, T. Brunner, and W. Brenig, *J. Chem. Phys.* **97**, 4453 (1992).

<sup>38</sup>I. Rips and E. Pollak, *Phys. Rev. A* **41**, 5366 (1990).

<sup>39</sup>D. J. Tannor and S. A. Rice, *Adv. Chem. Phys.* (Part 1), **70**, 441 (1988).

<sup>40</sup>J. Manz and C. S. Parmenter, *Chem. Phys.* **139**, 1 (1989).

<sup>41</sup>E. D. Potter, J. L. Herek, S. Pedersen, Q. Liu, and A. H. Zewail, *Nature* **355**, 66 (1992).